

Contract Order Number F61775-99-WE064

**SPC 99-4064 « Towards SiGe-Based Quantum Cascade
TeraHertz Lasers »**

**Final Report
(July 2000)**

J-M. Lourtioz, F. Julien, A. Chelnokov and S. Rowson
Institut d'Électronique Fondamentale
University of Paris Sud, Orsay (France)

20010817 064

AQ FOI-11-2349

REPORT DOCUMENTATION PAGE

Form Approved OMB No. 0704-0188

Public reporting burden for this collection of information is estimated to average 1 hour per response, including the time for reviewing instructions, searching existing data sources, gathering and maintaining the data needed, and completing and reviewing the collection of information. Send comments regarding this burden estimate or any other aspect of this collection of information, including suggestions for reducing this burden to Washington Headquarters Services, Directorate for Information Operations and Reports, 1215 Jefferson Davis Highway, Suite 1204, Arlington, VA 22202-4302, and to the Office of Management and Budget, Paperwork Reduction Project (0704-0188), Washington, DC 20503.

1. AGENCY USE ONLY (Leave blank)		2. REPORT DATE 26-October-2000	3. REPORT TYPE AND DATES COVERED Final Report	
4. TITLE AND SUBTITLE Towards SiGe-Based Quantum Cascade TeraHertz Lasers			5. FUNDING NUMBERS F61775-99-WE064	
6. AUTHOR(S) Jean-Michel L. Lourtioz				
7. PERFORMING ORGANIZATION NAME(S) AND ADDRESS(ES) CNRS-University of Paris-Sud Institut d'Electronique Fondamentale Orsay 91405 France			8. PERFORMING ORGANIZATION REPORT NUMBER N/A	
9. SPONSORING/MONITORING AGENCY NAME(S) AND ADDRESS(ES) EOARD PSC 802 BOX 14 FPO 09499-0200			10. SPONSORING/MONITORING AGENCY REPORT NUMBER SPC 99-4064	
11. SUPPLEMENTARY NOTES				
12a. DISTRIBUTION/AVAILABILITY STATEMENT Approved for public release; distribution is unlimited.			12b. DISTRIBUTION CODE A	
13. ABSTRACT (Maximum 200 words) This report results from a contract tasking CNRS-University of Paris-Sud as follows: The contractor shall measure resonator infrared (IR) modes using Fourier Transform Infrared Spectrometer (FTIR) and fabricate multiple quantum wells using PL to check for intersubband transitions. Initial studies will be aimed at demonstrating intersubband luminescence at terahertz (THz) frequencies in the valence band of SiGe(C) quantum structures. The next step will be to add multilayer active regions and carrier injectors for studying electroluminescence devices. In parallel, the cylindrical resonator issue will be addressed. Finally, the contractor will investigate the feasibility of cylindrical resonator electroluminescent and lasing devices.				
14. SUBJECT TERMS EOARD, Lasers, Semiconductor materials			15. NUMBER OF PAGES 9	
			16. PRICE CODE N/A	
17. SECURITY CLASSIFICATION OF REPORT UNCLASSIFIED	18. SECURITY CLASSIFICATION OF THIS PAGE UNCLASSIFIED	19. SECURITY CLASSIFICATION OF ABSTRACT UNCLASSIFIED	20. LIMITATION OF ABSTRACT UL	

NSN 7540-01-280-5500

Standard Form 298 (Rev. 2-89)
Prescribed by ANSI Std. Z39-18
298-102

I. Introduction :

This project aims to investigate building blocks of a future, but still hypothetical, unipolar quantum cascade TeraHertz laser based on SiGe(C)/Si quantum well structures. Today, optoelectronics is one of the last fields in the domain of advanced applications where silicon technology is not dominantly present. This situation mainly results from the lack of efficient silicon-based light emitters due to the indirect nature of optical band-to-band transitions in silicon and other group IV semiconductors. From this viewpoint, the use of inter-sub-band transitions in SiGe(C)/Si quantum wells represents a unique opportunity to bring the optical characteristics of group IV heterostructures closer to those of III-V heterostructures. As mid-infrared (or THz) laser action has recently been obtained using inter-sub-band transitions in a variety of III-V quantum well structures (namely, the famous quantum cascade laser [1] and its optically pumped version, the quantum fountain laser [2]), one may hope a similar laser action by using SiGe(C)/Si quantum well structures. However, group IV heterostructures and optical devices are much less mature than their III-V homologues both in terms of fabrication and characterization. Moreover, intersubband transitions in the SiGe(C)/Si system occur in the valence band, this specificity may lead to some difficulties. For all these reasons, it is imperative to deeply investigate the interband and intersubband properties of SiGe(C)/Si quantum well structures as well as to develop and characterize novel microresonators in silicon.

These were the two main directions of the work undertaken in this project. A spectroscopic analysis of intersubband absorption in SiGe(C)/Si quantum wells was first performed and followed by the investigation of new types of structures with large Ge content epitaxied on Ge(001). Microdisk resonators were then fabricated and characterized by Fourier Transform InfraRed (FTIR) spectroscopy. Numerical simulations were developed to evaluate the interest of incorporating photonic band gap (PBG) structures in the resonator. The possibility of high-Q whispering gallery modes was examined. Finally, the performances of a SiGe-based Quantum Cascade TeraHertz Laser were theoretically estimated. A significant part of these tasks was carried out in collaboration with the group of Pr. J. Kolodzey at the University of Delaware.

II. Studies of SiGe(C) Multi-Quantum Well Structures :

II.1 Infrared absorption spectroscopy :

Figure 1 (left) gives a schematic representation of intersubband transitions in a quantum well. In the case of interest where the well is formed by a thin SiGe(C) layer sandwiched in between two Si barriers, the band discontinuity mainly occurs in the valence band. Intersubband transitions within this band may involve heavy-hole (HH), light-hole (LH) and spin-orbit (SO) bound states as well as continuum states. In principle, intersubband transitions are p-polarized (i.e. the electric field is perpendicular to the layers). However, because of band-mixing effects in the valence band, the polarization selection rule is relaxed and s-polarized (i.e., in-plane) intersubband transitions can also occur. As the main drawback, band mixing also results in weaker strengths and larger widths of transitions.

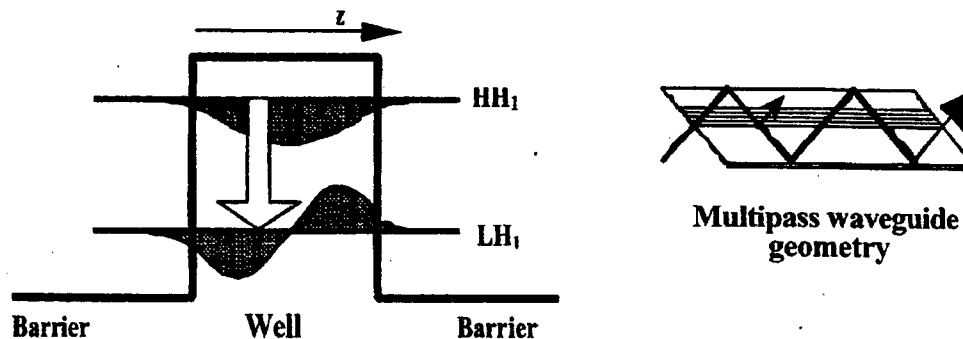


Figure 1. Left: schematic representation of an intersubband absorption transition in the valence band of a quantum well, Right: multi-pass waveguide geometry used for infrared absorption spectroscopy

Intersubband transitions can be directly probed by using different schemes of infrared absorption spectroscopy. The major requirement is to populate the ground subband (HH1 in fig.1). The technique we used to populate the subbands relied on optical pumping of interband transitions to generate photo-carriers in the conduction and valence bands. Because the intersubband and intrasubband relaxation times are much shorter than the band-to-band recombination times, the photocarriers accumulate in the ground valence subbands of the quantum wells. This photo-induced absorption technique was found to be well suited for intersubband spectroscopy of undoped structures [3]. The multi-pass waveguide configuration where the light enters the sample at normal incidence on a facet polished at a 45° angle (fig.1 right), was used for spectroscopic measurements since it allows a large absorption due to the excellent coupling of p-polarized light and to multiple passes within the active layer.

Figure 2 shows the experimental set-up. A Fourier transform InfraRed (FTIR) spectrometer is operated in the step-scan mode. A polarizer placed ahead of the multi-pass waveguide sample allows one to probe either the in-plane polarized absorption (s-polarization) or the absorption polarized perpendicular to the layers (p-polarization). An Ar^{++} or Ti:Sapphire pump laser beam is focused onto the sample surface. A chopper is used to modulate the pump intensity. The resulting changes in the IR sample transmission are detected using an IR detector and a lock-in amplifier. The photoinduced transmission spectrum ($\Delta T/T$) is obtained after Fourier transform. Intersubband absorptions as low as 10^{-5} can be detected using set-up.

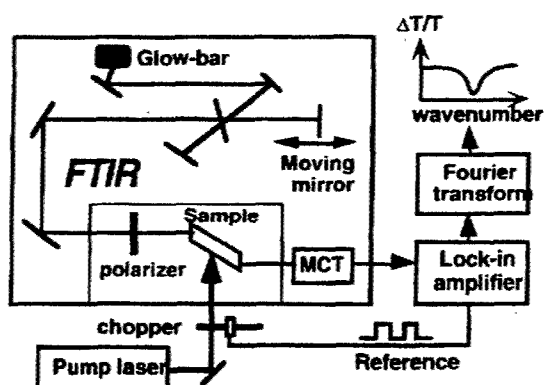


Figure 2. Experimental set-up for photo-induced intersubband absorption spectroscopy.

II.2 Intersubband absorption measurements on $\text{Si}_{0.5}\text{Ge}_{0.5}$ samples :

Optical intersubband transitions were characterized for multi-quantum well Si/SiGe structures with a large content of germanium. As a typical example of our measurements, figure 3 shows the photo-induced absorption spectroscopy of a multi-pass waveguide sample containing 20 undoped periods of 1.8 nm thick $\text{Si}_{0.5}\text{Ge}_{0.5}$ wells and 32 nm thick Si barriers. The pump excitation is provided by an Ar^{++} laser. The spectra for both p- and s-polarizations show resonances characteristic of hole intersubband absorptions in addition to significant free-carrier absorption. Energy calculations show that the only bound levels in the structure are the heavy-hole, light-hole and spin-orbit states, HH1, LH1 and SO1, respectively. The resonance at 115 meV is attributed to the HH1→LH1 transition while the s-polarized peak at 265 meV corresponds to the HH1→SO1 transition. Both transitions are allowed for carriers far from Brillouin zone center. As seen, significant s-polarized intersubband absorption is observed. However, one can notice that the p-polarized intersubband absorption is larger at low energies. It is confirmed that the intersubband resonances in the valence band are much broader than those observed in the conduction band of GaAs QWs due to the mixing between HH and LH bands far from Brillouin zone center and the consequent non-parabolicity of the hole subbands [4]. In spite of this, the oscillator strength of intersubband transitions remains large with an amplitude of about one tenth of that measured for GaAs/AlGaAs samples.

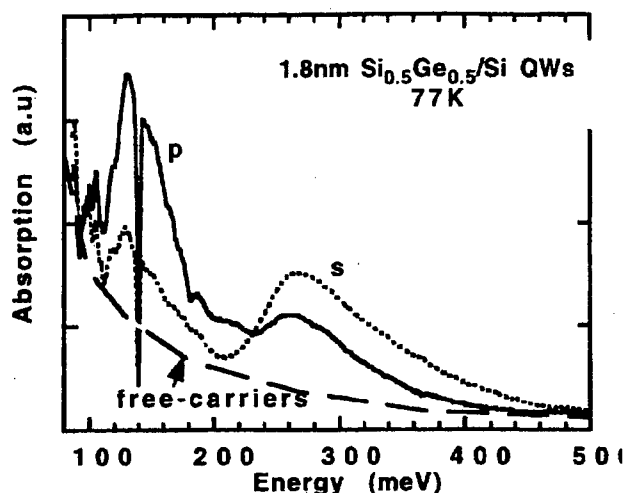


Figure 3. Photo-induced intersubband absorption spectroscopy at 77 K of undoped 1.8 nm thick Si_{0.5}Ge_{0.5} wells with Si barriers for p-polarization (full line) and s-polarization (dotted line). The free-carrier contribution is indicated by the dashed line.

II.3 Photoluminescence characterization of Ge_{1-y}C_y and Ge_{1-x-y}Si_xC_y samples on Ge substrates :

The diversification of group IV heterostructures allows a larger flexibility in the design of optical devices. Carbon incorporation into Si and SiGe has been studied by several groups during the last years. One objective was to compensate the compressive strain in SiGe layers epitaxied on silicon substrate induced by Ge. Dislocation free SiGeC layers thicker than SiGe ones were grown with potential detection and SiGe(C) optical waveguide applications. Another interest stemmed from the possibility of varying the valence and conduction band offsets. For instance, about 20 meV bandgap increase per carbon percent has been measured for SiGeC layers with less than 2% carbon.

In this work, we studied new types of heterostructures such as Ge_{1-y}C_y and Ge_{1-x-y}Si_xC_y epitaxied on Ge(001) substrates with ($0 < y < 0.001$) and ($0 < x < 0.05$). The samples were grown at the University of Delaware by using low temperature ($\sim 275^\circ\text{C}$) molecular beam epitaxy. In spite of low y values, this carbon fraction exceeds by 10 orders of magnitude the solubility limit of C in bulk germanium. High resolution X-ray diffraction revealed that the layers were pseudomorphic and had high crystalline quality and interface abruptness. The optical quality of the samples was tested via PhotoLuminescence (PL) experiments at the University of Orsay. Figure 4. shows the photoluminescence spectra of epitaxial Ge (dotted line) and pseudomorphic

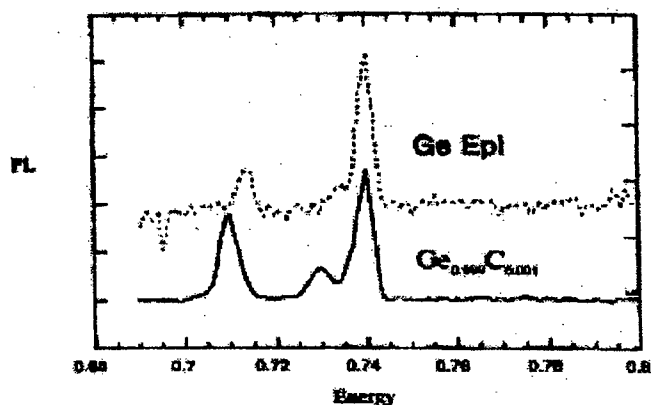


Fig. 4: Photoluminescence spectra of epitaxial Ge (dotted line) and pseudomorphic Ge_{0.9995}C_{0.0005} on Ge (solid line)

$\text{Ge}_{0.9995}\text{C}_{0.0005}$ on Ge (solid line). As the major result, band-edge photoluminescence is observed for pseudomorphic $\text{Ge}_{1-y}\text{C}_y$, suggesting that this heterostructure system brings potential new strained layer opto-electronic epitaxial system. Indeed, the high energy peak at 740 meV is assigned to the (non-phonon) NP recombination line. In addition, the alloy layer exhibits TA and LA phonon-assisted recombination lines which are slightly shifted as compared to those measured on epitaxial Ge. The results of the collaborative work between the University of Delaware and the University of Orsay were presented at the NAMBE Conference in Banff (Oct. 99) [5].

III. Microdisk resonator fabrication, characterization and modeling:

III. 1 Fabrication of microdisk resonators on silicon :

The fabrication of microdisk resonators on silicon required several steps of material processing. Using chemical vapor deposition (CVD) in the group of D. Bensahel at CNET in Grenoble, the first step was to grow $7\text{ }\mu\text{m}$ of p-type B-doped Si to serve as the pedestal, on a 200 mm diameter Si substrate. Next, $3\text{ }\mu\text{m}$ of bulk SiGe alloy were grown as the resonator material. The Ge content in the alloy was 5 atomic %. The CVD system was an ASM Epsilon III reactor. The B-doping of the pedestal layer allows the use of a selective etch to create a micro-disk. The layers were etched to form cylindrical pillars as shown in the SEM figure below (fig.5).

The etching steps were optimized to obtain the final structure with sufficient undercutting to produce a microdisk surrounded by air on 3 sides. The first etchant used was XeF_2 , an unstable solid that sublimates in a vacuum and quickly etches Si, at a rate of $1\text{ }\mu\text{m}$ in 4.5 min. We calibrated the etch rates versus composition for our layers. The XeF_2 etch is isotropic, with insufficient undercutting to allow the microdisk to be surrounded by air on 3 sides. To create undercutting, we used a wet chemical selective etch that etched our B doped pedestal, but not the microdisk. The selective etches we used included $\text{NH}_4\text{OH}:\text{H}_2\text{O}_2:\text{H}_2\text{O}$ (1:1:4) which etches SiGe but stops on Si, and $\text{HF}:\text{HNO}_3:\text{CH}_3\text{COOH}$ (1:3:10) which etches heavily doped p+ Si.

The optical lithography as well as a large part of the etching process was performed at the University of Delaware. The final etch was performed at the University of Orsay to minimize the pedestal diameter. Fig. 5 shows a micrograph of the smallest microdisk resonators obtained after the different steps of fabrication. The disk diameter is between 30 and $50\text{ }\mu\text{m}$, the disk thickness is $\sim 2\text{--}3\text{ }\mu\text{m}$ and the pedestal height is $\sim 7\text{ }\mu\text{m}$.

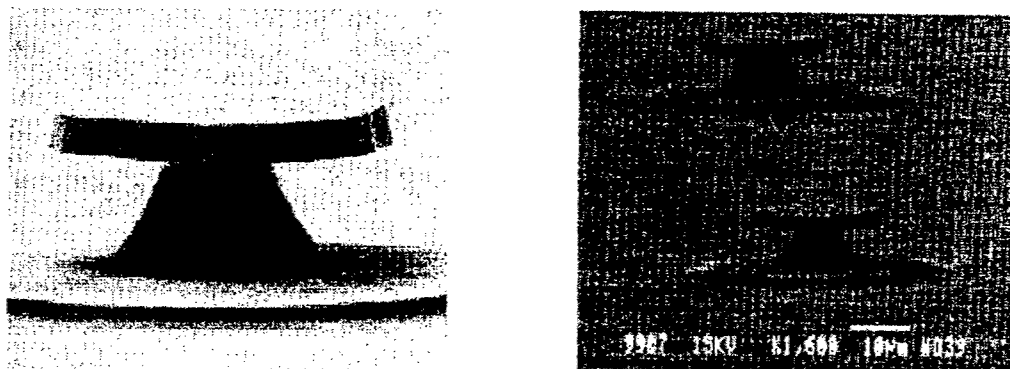


Fig. 5: Micrographs of the smallest microdisk resonators ($0\text{--}30\text{--}50\text{ }\mu\text{m}$) obtained by selective etching of silicon

III. 2 Infrared characterization of microdisk resonators on silicon :

The microdisks were optically characterized using a FTIR spectrometer equipped with a microscope. This equipment allowed wideband measurements, from 1.5 to $14\text{ }\mu\text{m}$ wavelength, with a spatial resolution of $\sim 30\text{ }\mu\text{m}$. In contrast, one only had access to vertical resonant modes since the microdisk resonators could only be coupled at normal incidence (from top to bottom in fig.5). In fact, the coupling to whispering gallery modes requires a waveguide geometry. On the

other hand, radial modes cannot be observed since they presently suffer from strong coupling to the layer (leaky modes).

Figure 6 shows a typical reflexion spectrum measured between 3000 cm^{-1} ($\lambda \sim 2.9\mu\text{m}$) and 10000 cm^{-1} ($\lambda \sim 1\mu\text{m}$) for the disks of fig. 5. One clearly observes reflexion maxima and minima associated to the presence of micro-resonators. Actually, two resonators are present, the $2\text{-}3\mu\text{m}$ thick SiGe microdisk itself and a $\sim 7\mu\text{m}$ air resonator delimited by the bottom surface of the microdisk and the upper substrate surface. The separation between two successive reflexion maxima (or minima), $\Delta\sigma = 350\text{ cm}^{-1}$, should correspond to the free spectral range of the composite resonator. Indeed, one finds an effective resonator length $L_{\text{eff}} = 1/2\Delta\sigma \sim 14\mu\text{m}$ in agreement with the overall optical thickness of the composite resonator (microdisk + air resonator).

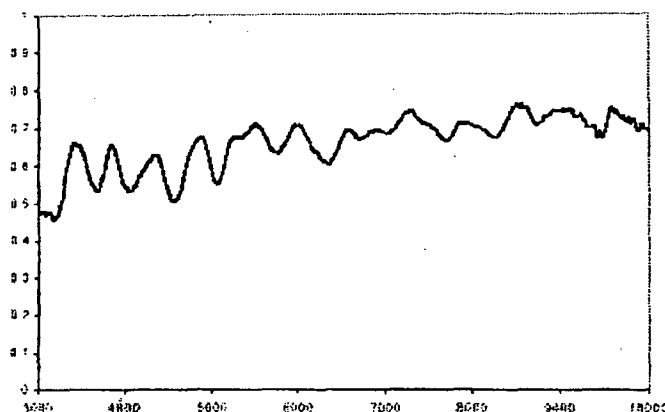


Fig. 6: Typical reflexion spectrum of microdisk resonators measured at normal incidence

III. 3 Modeling of microdisk resonators :

The reflection (or transmission) spectra measured at normal incidence (fig.6) were simulated using a standard multi-layer model including the two resonators previously mentioned (microdisk and air resonator). A satisfactory agreement was obtained between calculations and experiments.

A waveguide propagation model was separately developed to calculate the radial modes in the microdisk and design waveguide geometries for coupling the infrared light to the whispering gallery modes. It was shown that the microdisk thickness should be increased to $\sim 5\mu\text{m}$ to allow the propagation of whispering gallery modes at terahertz frequencies ($\lambda \sim 10\mu\text{m}$). Moreover, the pedestal diameter must be minimized to reduce the mode coupling to the substrate. A second improvement is to maximize the refractive index step between the microdisk and its pedestal.

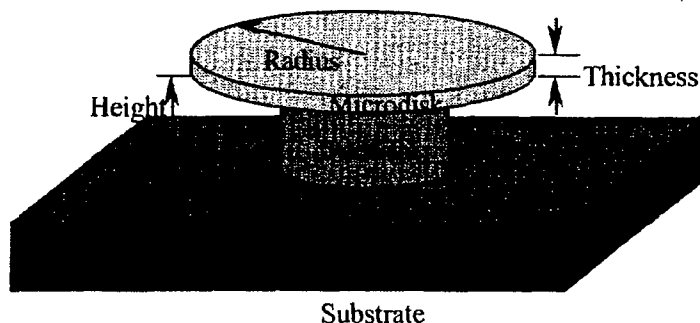


Figure 7 : Schematic representation of the microdisk resonator used in electromagnetic simulations

Figure 7 shows the idealized microdisk geometry used in electromagnetic simulations. For realistically optimized microdisk parameters, quality factors between ~ 100 and ~ 5000 were

predicted depending on the resonator mode number. The loss due to the coupling between the waveguide and whispering gallery modes was presently neglected.

III. 4 Interest of photonic band gap structures :

In order to reach higher Q-factors, we investigated the incorporation of two-dimensional (2D) photonic bandgap structures in the microdisk resonators. Usually, a 2D photonic crystal is fabricated by etching a periodic lattice of holes in a high-permittivity material like silicon. In the photonic bandgaps (the wavelength domains where light propagation is forbidden), the photonic crystal theoretically behaves as a perfect reflector. Very small resonators at the light wavelength scale can be obtained by inserting defects of periodicity in the photonic crystal (for instance, missing holes).

Macroporous silicon- based photonic crystals were fabricated at the University of Orsay in parallel to this work [6]. Figure 8 (left) shows the extreme regularity and very high aspect ratio of these bulk photonic structures. A full PBG was measured around $1.5 \mu\text{m}$ for the parameter values of fig.8. Actually, the PBG center wavelength could be tuned over a wide range by changing the lattice period [6]. Using a photonic crystal with a PBG centered at $\sim 7 \mu\text{m}$, a reflectivity higher than 98% was measured for the TE polarization of the incident field. Indeed, these results encouraged us to combine photonic bandgap structures and microdisk resonator for Q-factor improvement.

Figure 8 (right) shows the microdisk resonators with annular PBGs that were numerically simulated in this work. The presence of an annular PBG determines a ring resonator whose Q-factor can be higher than that of standard microdisk resonators. Again, the coupling between the linear waveguide and ring resonator modes was assumed to be lossless in the calculations. The microdisk material was also assumed to be lossless. As the major result, it was found that for a given microdisk size, the Q-factor could be increased by more than 20 with the incorporation of photonic structures. In other words, Q-factors larger than 10^5 are predicted for PBG ring resonators in the mid-infrared.

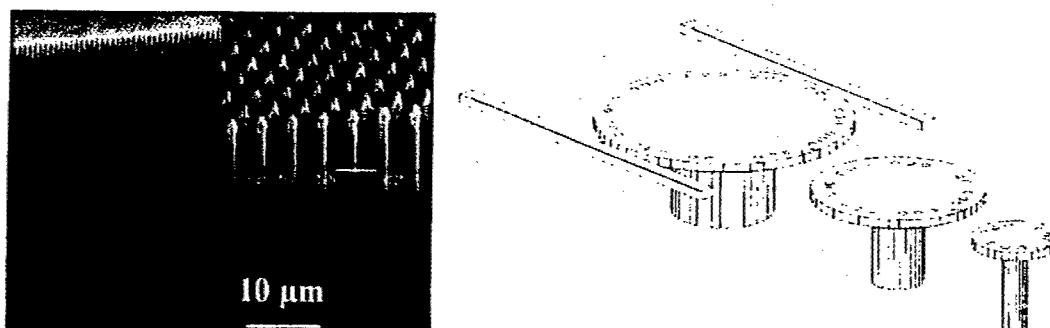


Figure 8 : (left) : 2D photonic crystal fabricated at IEF (Orsay) using the macroporous silicon technique (photo-electrochemistry of silicon substrates in the low-level n-doping case). The triangular lattice periodicity is $\sim 660\text{nm}$, the pore diameter is $\sim 380\text{nm}$, the pore depth is $\sim 50\mu\text{m}$.

The insert shows an exploded view of the crystal.

(right) : schematic representation of the microdisk resonators with annular PBG structures used in the electromagnetic simulations. The different sizes correspond to different resonator selectivities.

Linear waveguides are used to couple the whispering gallery modes.

IV. Summary and laser predictions:

In summary, different results have been obtained that represent important steps toward a unipolar SiGe laser emitting at teraHertz frequencies.

In the first part of this work, optical intersubband transitions at these frequencies have been studied in SiGe/Si multiquantum well structures using photo-induced absorption spectroscopy. These transitions are somewhat weaker than their homologues in III-V quantum wells, but the relaxation of polarization selection rules may lead to simpler excitation schemes (in-plane

excitation). New types of heterostructures (GeC on Ge) have been fabricated and characterized. An additional flexibility can thus be envisaged in the design of quantum well structures and optical devices based on group IV materials.

In the second part of this work, microdisk resonators including SiGe layers have been fabricated on silicon substrates. The results of first characterizations (SEM micrographs and optical measurements) are very encouraging. An electromagnetic model has been implemented to evaluate the optimal characteristics of whispering gallery modes. For realistic values of the microdisk parameters, resonator Q-factors of ~ 5000 can be reached. A supplementary optimization has been proposed by incorporating photonic bandgap structures in the microdisk. Q-factors larger than 10^5 are predicted for this novel resonator configuration.

Considering such resonator performances and assuming negligible optical and electrical laser loss, one can estimate the ultimate performances of a hypothetical SiGe inter-sub-band laser as follows. First, the internal quantum efficiency per quantum well is given by: $\eta = (1/\tau_{\text{rad}})/(1/\tau_{\text{tot}}) = 40 \text{ ps}/1 \text{ } \mu\text{sec} = 4 \times 10^{-5}$, where τ_{tot} is the inter-sub-band level lifetime and τ_{rad} , the radiative lifetime. If the efficiency simply scales with the number of quantum wells, the laser internal efficiency can then reach $\sim 2 \times 10^{-4}$ (0.14%) for a reasonable number of quantum wells (~ 35). Next, for a typical current density $J = 10,000 \text{ A cm}^{-2}$ in pulsed mode, the flux of carriers (holes) in the upper level will be: $N = J \tau_{\text{tot}}/q = 2.5 \times 10^{12} \text{ cm}^{-2}$ holes, leading to a number of emitted photons $N/\tau_{\text{rad}} = 2.5 \times 10^{18} \text{ s}^{-1} \text{ cm}^{-2}$ per unit time and per well. This will correspond to an optical power density $I_{\text{out}} = \hbar\omega_p N/\tau_{\text{rad}} = 16.4 \text{ mW cm}^{-2}$ per well for a photon energy $\hbar\omega = 41 \text{ meV}$ (i.e., a 10 THz laser frequency). Finally, in a single 500 μm diameter microdisk with 35 quantum wells and an active area of $1.26 \times 10^{-3} \text{ cm}^2$, one expects to have an optical power $P_{\text{out}} = 0.7 \text{ mW}$.

V. References :

- [1] J. Faist, F. Capasso, D. L. Sivco, C. Sirtori, A. L. Hutchinson and A. Y. Cho, *Quantum cascade laser: an intersubband semiconductor laser operating above liquid nitrogen temperature*, Electron. Lett. **30**, 865 (1994).
- [2] O. Gauthier-Lafaye, P. Boucaud, F.H. Julien, S. Sauvage, S. Cabaret, J-M. Lourtioz, V.Thierry-Mieg, R. Planel, "Long-wavelength 15.5 μm unipolar semiconductor laser in GaAs quantum wells", Appl. Phys. Lett. **71**, 3619-3621 (1997).
- [3] D. D. Yang, F. H. Julien, J.-M. Lourtioz, P. Boucaud, and R. Planel, *First demonstration of room-temperature intersubband-interband double-resonance spectroscopy of GaAs/AlGaAs quantum wells*, IEEE Photon. Technol. Lett. **2**, 398 (1990).
- [4] E. Corbin, K.B. Wong and M. Jaros, *Absorption in p-type Si-SiGe quantum well structures*, Phys. Rev. **B 50**, 2339 (1994).
- [5] M.W. Dashiell, J. Kolodzey, P. Boucaud, Vy Yam, J-M. Lourtioz « *Heterostructures of pseudomorphic $\text{Ge}_{1-y}\text{C}_y$ and $\text{Ge}_{1-x-y}\text{Si}_x\text{C}_y$ alloys grown on Ge(001) substrates* », North American Molecular Beam Epitaxy (NAMBE) Conference, Banff, Oct. 1999.
- [6] S. Rowson, A. Chelnokov and J-M. Lourtioz, "Two-dimensional photonic crystals in macroporous silicon: from mid-infrared (10 μm) to telecommunication wavelengths (1.3-1.5 μm)", IEEE Journal of Lightwave Technol. JLT **17**, pp. 1989-1995 (Novembre 1999)